Development 138, 1631-1641 (2011) doi:10.1242/dev.057208

Distinct cytoskeleton populations and extensive crosstalk control *Ciona* notochord tubulogenesis

Bo Dong, Wei Deng and Di Jiang*

SUMMARY

Cell elongation is a fundamental process that allows cells and tissues to adopt new shapes and functions. During notochord tubulogenesis in the ascidian *Ciona intestinalis*, a dramatic elongation of individual cells takes place that lengthens the notochord and, consequently, the entire embryo. We find a novel dynamic actin- and non-muscle myosin II-containing constriction midway along the anteroposterior aspect of each notochord cell during this process. Both actin polymerization and myosin II activity are required for the constriction and cell elongation. Discontinuous localization of myosin II in the constriction indicates that the actomyosin network produces local contractions along the circumference. This reveals basal constriction by the actomyosin network as a novel mechanism for cell elongation. Following elongation, the notochord cells undergo a mesenchymal-epithelial transition and form two apical domains at opposite ends. Extracellular lumens then form at the apical surfaces. We show that cortical actin and *Ciona* ezrin/radixin/moesin (ERM) are essential for lumen formation and that a polarized network of microtubules, which contributes to lumen development, forms in an actin-dependent manner at the apical cortex. Later in notochord tubulogenesis, when notochord cells initiate a bi-directional crawling movement on the notochordal sheath, the microtubule network rotates 90° and becomes organized as parallel bundles extending towards the leading edges of tractive lamellipodia. This process is required for the correct organization of actin-based protrusions and subsequent lumen coalescence. In summary, we establish the contribution of the actomyosin and microtubule networks to notochord tubulogenesis and reveal extensive crosstalk and regulation between these two cytoskeleton components.

KEY WORDS: Notochord, Tubulogenesis, *Ciona intestinalis*, Cell elongation, Lumen formation, Cell migration, Actomyosin, Microtubule, ERM

INTRODUCTION

Multicellular tubes and tubular networks play crucial roles in embryogenesis, organogenesis and adult physiology. The processes of cell shape change, lumen formation and cell migration during tubulogenesis have been studied in different model systems (Baer et al., 2009; Bryant and Mostov, 2008; Chung and Andrew, 2008; Hogan and Kolodziej, 2002; Lu and Werb, 2008; Lubarsky and Krasnow, 2003). However, much remains unknown concerning the molecular mechanisms underlying these cellular processes.

The cytoskeleton, especially the actin/microtubule network, is essential for cell shape change in nearly every morphogenetic process, including tubulogenesis (Gervais and Casanova, 2010; Pollard and Cooper, 2009; Strilic et al., 2009). Cell shape changes generally result from the polymerization of actin filaments and their interaction with the motor protein myosin, which causes the actin filaments to contract. Actomyosin contraction provides the primary physical force driving cell shape changes in cytokinesis, cell migration and apical constriction. Polarized intracellular trafficking has been implicated in lumen formation during tubulogenesis. Secretory vesicles carrying both apical membrane and luminal matrix are transported towards apical/luminal membrane along microtubules and actin filaments by different classes of motor, including kinesins, dyneins and unconventional myosins (Gobel et al., 2004; Hirokawa et al., 2009; Jerdeva et al., 2005; Massarwa et al., 2009; O'Brien et al., 2002; Ross et al., 2008; Strilic et al., 2009; Tsarouhas et al., 2007). Cell migration is accomplished by the activity of actin filament-based lamellipodia. The actin filaments in migrating cells are highly dynamic, spatially and temporally regulated, and well coordinated with other cellular components including microtubules (Etienne-Manneville, 2004).

The ascidian notochord, which consists of only 40 post-mitotic cells, presents an ideal model with which to study cell shape changes and tubulogenesis. During notochord tube formation in *Ciona intestinalis*, individual notochord cells elongate along their anterior/posterior (A/P) axis. This elongation is followed by an unusual mesenchymal-epithelial transition. Apical/luminal domains form and extracellular lumens emerge at the opposite ends of each cell. As the lumens enlarge, each notochord cell initiates a bi-directional crawling movement, which results in the merging of two apical domains, the conversion of the cell to an endothelial-like morphology, and the fusion of the neighboring lumens (Cloney, 1964; Dong et al., 2009; Jiang and Smith, 2007; Miyamoto and Crowther, 1985).

In this study, we use live imaging together with various cytoskeleton disruptors, including small chemical inhibitor, dominant-negative and gene knockdown approaches, to explore the role of cytoskeleton elements and their interaction in cell elongation, extracellular lumen formation and lumen fusion during *Ciona* notochord tubulogenesis. First, we describe the existence of a basal constriction at the equator of notochord cells during cell elongation. This constriction is associated with a highly dynamic actomyosin ring. Both actin and myosin II are required for the formation of the constriction and cell elongation. Next, we show that an apical cortical actin/microtubule network is required for lumen formation

Sars International Centre for Marine Molecular Biology, University of Bergen, Thormøhlensgate 55, N-5008 Bergen, Norway.

*Author for correspondence (di.jiang@sars.uib.no)

Accepted 2 February 2011

in the notochord. The *Ciona* ortholog of ezrin/radixin/moesin (ERM) is essential for lumen development. Finally, we show that later, when notochord cells begin to crawl, the microtubule network makes a 90° rotation and extends into the leading edges of lamellipodia. This process is required for the formation and orientation of single actin-based protrusions at each cell end and for subsequent lumen fusion.

MATERIALS AND METHODS

Animals and embryos

Adult *Ciona intestinalis* were collected from Grimstadfjorden, Norway. Eggs were removed and mixed in seawater with sperm from other individuals. After fertilization, the embryos were cultured at 16°C.

DNA electroporation and morpholino microinjection

Electroporation was performed as described previously (Dong et al., 2009). Ci-ERM morpholino (MO) (5′-GTTTCCAAACATTATTACATCACAG-3′) was a gift from Hiroki Takahashi (Hotta et al., 2007). Microinjection was carried out as described previously (Satou et al., 2001) with some modifications. The unfertilized eggs were injected with a mixture of 20 fmoles MO and Rhodamine-dextran or Fast Green as dye. A standard control MO from GeneTools was used as negative control.

Plasmid construction

The GFP and mCherry-hActin (which expresses human actin) expression clones were described previously (Dong et al., 2009). *Ciona* ERM expression construct ERM-EGFP (Hotta et al., 2007) was a gift from Hiroki Takahashi. *Ciona* myosin II light chain (MLC) was amplified with primers 5′-ATGTCGAGCCGACGAACTAAA-3′ and 5′-CTAAATGTCATCTTTT-TCTTTAGCG-3′. The talin A I/LWEQ module was amplified from *Ciona* talin A I/LWEQ dsRed construct (Singiser and McCann, 2006) with primers 5′-ATTTTGGAAGCCGCAAAATCA-3′ and 5′-TTAATCGGATTCAG-AATCATC-3′. Lifeact-mEGFP was amplified from pTH-Ubi-Lifeact-mEGFP (Vidali et al., 2009) with primers 5′-CAGAAAAAATG-GGTGTCGCAGATTTGATCAAG-3′ and 5′-TTACTTGTACAGCTCG-TCCATGCC-3′. UtrCH was amplified from pCS2-eGFP-UtrCH (1-161) (Burkel et al., 2007) with primers 5′-GGCGCCTCCGGAACCATG-3′ and 5′-CTCGAGTTAGTCTATGGTG-3′. Dominant-negative ERM (ERM-DN) containing the N-terminal 344 amino acids (including the FERM domain) was amplified with primers 5′-CAGAAAAAATGTTTGGAAACAA-AGGAACA-3′ and 5′-TCTTTCCAGTTCCTTCTTATGTTTTTCC-3′. All PCR products were cloned into the pCR8/GW/TOPO vector (Invitrogen) to obtain entry clones. The ensconsin-3×GFP entry clone was a gift from Patrick Lemaire (Roure et al., 2007). These entry clones were used to generate notochord expression constructs using the destination vectors (Dong et al., 2009) *Minos*-B3-eBra-bpFOG-B5::Kozak-mCherry-R1-*ccd*B/CmR-R2 (for mCherry-MLC, mCherry-talin A and mCherry-UtrCH), *Minos*-B3-eBra-bpFOG-B5::Kozak-R1-*ccd*B/CmR-R2 (for ensconsin-3×GFP and Lifeact-mEGFP), and *Minos*-B3-eBra-bpFOG-B5::R1-*ccd*B/CmR-R2-tGFP (for ERM-DN-tGFP) by the Gateway cloning method (Invitrogen).

Immunohistochemistry and phalloidin staining

Dechorionated embryos were fixed with a mixture of 2% formaldehyde and 0.2% glutaraldehyde as previously described (Foe and von Dassow, 2008). Fixed embryos were stained with 1:500 anti-α-tubulin antibody (12G10, DSHB) and TRITC anti-mouse IgG secondary antibody (Sigma, T-5393), then counterstained with 3 units/ml BODIPY FL phalloidin (Invitrogen, B607).

Drug treatments

Blebbistatin (Sigma, B0560), latrunculin B (Sigma, L5288), nocodazole (Sigma, M1404) and Ro-31-8220 (Calbiochem, 557520) were dissolved in DMSO. Final concentrations and treatment periods are described in the Results. All inhibitor treatments were repeated at least three times.

Imaging

Differential interference contrast (DIC) images were taken with a Nikon Eclipse (E800) microscope equipped with a 40× objective (NA 1.00) and a SPOT RtKE CCD camera (Diagnostic Instruments). Confocal images were taken with a Leica TCS SP5 confocal laser-scanning microscope equipped with 40× oil-immersion and 63× water-immersion objectives (NA 1.25 and 1.40, respectively) at 1 μm intervals. Image analysis and three-dimensional reconstruction were performed using Leica TCS SP5 LAS AF software packages.

RESULTS

Notochord cell elongation and basal constriction at the early stage of tubulogenesis

Following convergent extension, the *Ciona* notochord continues to elongate ~3-fold (Dong et al., 2009; Jiang and Smith, 2007; Miyamoto and Crowther, 1985). This post-convergent extension elongation is accomplished by dramatic changes in cell shape and arrangement between 14 and 36 hours post-fertilization (hpf). In the initial phase (14-20 hpf), notochord elongation resulted from elongation of the constituent cells: average individual notochord cells elongated ~2-fold, while the diameter of each cell decreased by ~1.4-fold (Fig. 1A). By 20 hpf, notochord cell length was approximately equal to cell diameter and cell elongation stopped. At this time, each notochord cell possesses three membrane domains: apical/luminal, lateral and basal (Dong et al., 2009) (Fig. 1A). By DIC and confocal microscopy, we found that a constriction appeared on the basal surface of each notochord cell, midway between the anterior and posterior ends (designated as the cell equator), at 16 hpf. The furrow resulting from the constriction progressively deepened and reached its greatest depth at 18 hpf (Fig. 1B,C). The basal furrow subsequently regressed at 20 hpf and disappeared by 22 hpf.

Dynamic actin and myosin ring at the basal furrow during notochord cell elongation

The spatiotemporal correlation of the basal furrow and cell elongation prompted us to investigate its structure and function. The basal furrow resembles, to some degree, the cleavage furrow during cytokinesis, where an actomyosin contractile network drives furrow ingression (Barr and Gruneberg, 2007). We investigated the subcellular localization of actomyosin filaments in notochord cells from 15 to 22 hpf. We expressed an mCherry-hActin marker under a notochord-specific promoter (Dong et al., 2009). Electroporation of this DNA construct into *Ciona* gave mosaic expression, as illustrated in Fig. 2A. The majority of actin filaments in all marker-expressing cells localized to the lateral surfaces of the notochord cells (white arrowheads in Fig. 2A-C). These actin filaments were most likely associated with adherens junctions. At 15 hpf, a second population of actin filaments emerged at the equator (white arrows in Fig. 2A). A projection of confocal images showed that these actin filaments formed a ring around the circumference of the notochord cells (white arrows in Fig. 2A′-C′). Onset of the actin ring preceded the morphological basal furrow by ~1 hour. The actin ring widened and intensified between 18 and 20 hpf (Fig. 2B′,C′). By 22 hpf, both the actin ring and basal furrow had disappeared (Fig. 2D,D′). The actin ring also stained with phalloidin at 17 hpf (see Movie 1 in the supplementary material).

Non-muscle myosin II, labeled with *Ciona* non-muscle myosin II light chain (MLC) fused with mCherry, localized to a circumferential belt in the same region as the actin ring at 15 hpf (Fig. 2E,E′). The width of the myosin belt increased significantly from 18 to 20 hpf, then decreased from 20 to 21 hpf, before the belt disappeared at 22 hpf (Fig. 2F-H′; data not shown). Intriguingly, the myosin belt was not uniform along the circumference, but was interspersed with less intensely labeled regions (yellow arrows in Fig. 2E′,F′).

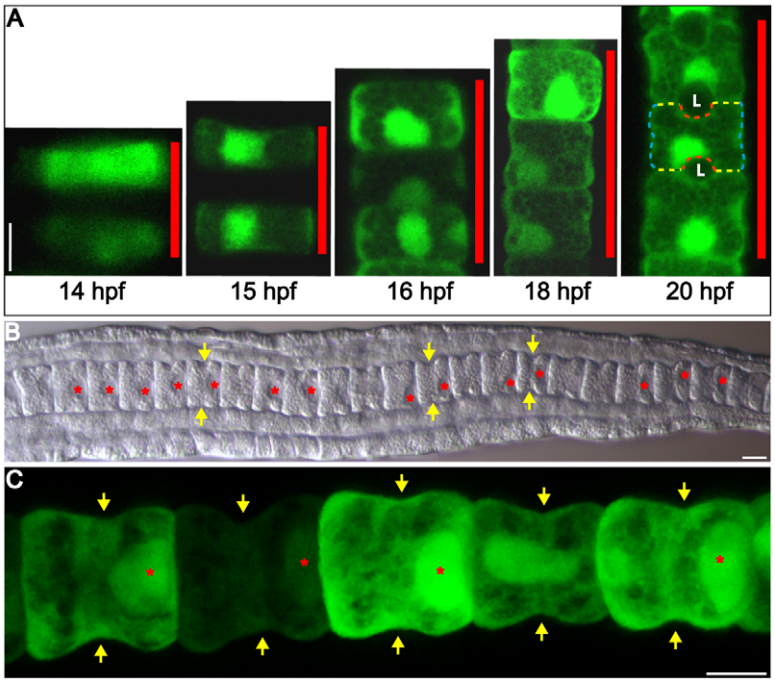

Fig. 1. Notochord cell elongation and basal constriction at the early stage of tubulogenesis in *Ciona intestinalis*. (**A**) Longitudinal sections of notochord segment mosaically expressing GFP. Red bars indicate lengths of three consecutive cells. Red, yellow and blue dashed lines indicate the apical/luminal, lateral and basal domains, respectively. L, lumen. (**B**) DIC image of a notochord segment at 18 hpf. (**C**) Projection of confocal images of notochord cells mosaically expressing GFP at 18 hpf. Yellow arrows indicate basal furrows/constrictions; red asterisk indicates nucleus. Scale bars: 10 μm.

Both actin and non-muscle myosin II are required for basal constriction and notochord cell elongation

Based on the dynamic distribution of the actomyosin network at the basal furrow, we reasoned that the actomyosin ring could constrict the notochord cell at the equator and drive cell elongation. To test this hypothesis, we used latrunculin B to disrupt actin polymerization and blebbistatin to inhibit the non-muscle myosin II ATPase. The embryos were treated at 16 hpf with latrunculin B and blebbistatin, respectively, for 2 hours. Whereas notochord cells in control (DMSO-treated) embryos formed constrictions (yellow arrow in Fig. 3A) and elongated, no constriction was observed with latrunculin B or blebbistatin treatment and cells retained a columnar shape (Fig. 3B,C). We further examined cytoskeleton components in drug-treated notochord. After latrunculin B treatment, both equatorial and adherens junction-associated actin filaments were disrupted (Fig. 3G). The majority of actin formed clusters ectopically in the cytoplasm (yellow arrowheads in Fig. 3G). Unexpectedly, microtubules, labeled with the microtubule-binding protein ensconsin-3×GFP (Roure et al., 2007), were also severely disrupted (Fig. 3H). A population of microtubules normally associated with the presumptive apical/luminal domain (magenta arrows in Fig. 3E) was lost, and the majority of microtubules formed thick bundles (magenta arrowheads in Fig. 3H). Interestingly, some MLC accumulated at the equator after latrunculin B treatment (Fig. 3I). Blebbistatin treatment did not disrupt the normal organization of actin (Fig. 3J) and microtubules (Fig. 3K), whereas it sufficiently and preferentially abolished the basal equatorial localization of MLC (Fig. 3L). Our data suggest that the actomyosin network at the furrow is essential for basal constriction and cell elongation.

The polarized distribution of microtubules is actin polymerization-dependent and is required for extracellular lumen expansion

One of the remarkable cellular processes that occur during *Ciona* notochord tubulogenesis is lumen formation, which begins at ~18 hpf (Dong et al., 2009). Disruption of actin filaments at 16 hpf not only arrested cell elongation, but also blocked lumen formation (data not shown) and the polarized distribution of microtubules (Fig. 3H). This demonstrates that the polarized distribution of microtubules is actin polymerization-dependent and suggests that the disruption of apical domain-associated microtubules might cause the failure of lumen formation following latrunculin B treatment. We therefore investigated the role of microtubules in lumen formation. During cell elongation, microtubules were organized uniformly at the basal cortex (16 hpf, Fig. 4A,A′; see also Movie 2 in the supplementary material), with the majority arrayed in an orientation parallel to the circumference of the cell (red arrows in Fig. 4A′). At the onset of lumen formation (18 hpf; Fig. 4B,B′; see Movie 3 in the supplementary material), while the circumferential microtubules persisted (red arrows in Fig. 4B′), a significant population of microtubules became concentrated at the center of the lateral surface where the lumens emerged (magenta arrows in Fig. 4B,B′). These microtubules remained in the apical/luminal cortex throughout the lumen formation process (magenta arrows in Fig. 4C-D), juxtaposing with large extracellular lumens. Anti-α-tubulin staining confirmed the presence of apical cortical microtubules (see Fig. S1 in the supplementary material). At 23 hpf, when notochord cells began crawling, a subset of microtubules reoriented along the A/P axis and extended towards the leading edge protrusions (see below).

The apical localization of microtubules suggested a potential contribution to lumen formation. We used the microtubule inhibitor nocodazole to test this hypothesis. Embryos were treated with 40 μM nocodazole before lumen formation at 17.5 hpf (Fig. 5A). After 4 hours, whereas large extracellular lumens formed in control (DMSO-treated) embryos (Fig. 5B), lumens in nocodazole-treated embryos were significantly smaller (Fig. 5C). The smaller lumens eventually developed into large lumens, although over a longer period than normal (data not shown). We confirmed that microtubule filaments were efficiently disassembled in nocodazole-treated embryos after 1 hour (compare Fig. 5D with Fig. 4B). Surprisingly, the disruption of microtubules caused an ectopic enrichment of actin filaments at the presumptive apical domains

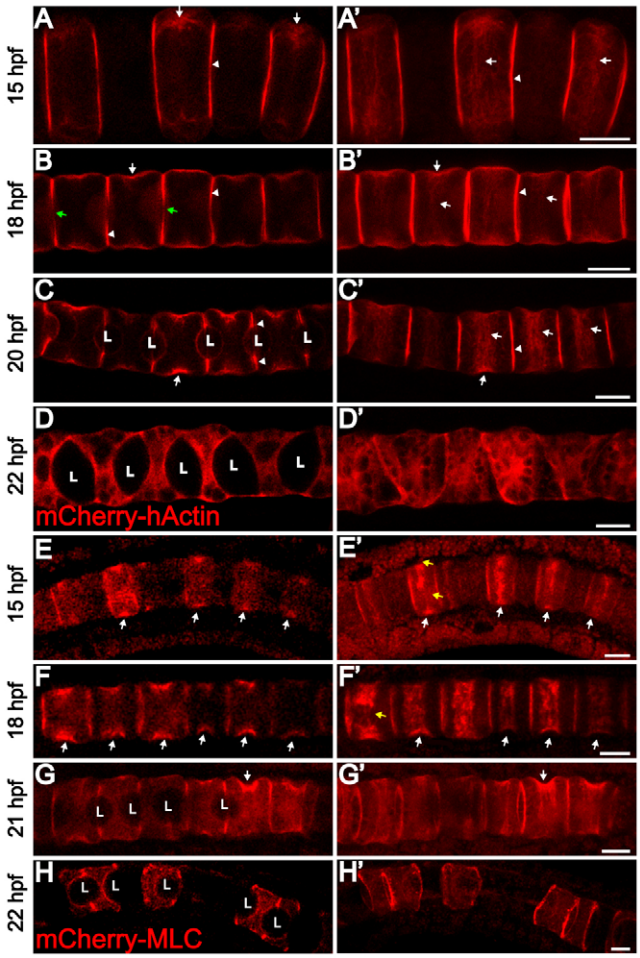

Fig. 2. Dynamics of the actomyosin ring in the basal furrow during notochord cell elongation. (**A-D′**) Median confocal sections (A-D) and projections (A′-D′) of *Ciona* notochord cells mosaically expressing mCherry-hActin at 15, 18, 20 and 22 hpf. White arrow indicates actin filament ring; white arrowhead indicates adherens junction-associated actin; green arrow indicates prospective apical/luminal domain. (**E-H′**) Median confocal sections (E-H) and projections (E′-H′) of notochord cells labeled with mCherry-myosin II light chain (MLC) at 15, 18, 21 and 22 hpf. White arrow indicates myosin belt; yellow arrow indicates where the myosin belt is broken. L, lumen. Scale bars: 10 μm.

(the center of the lateral interface; white arrows in Fig. 5E) where, at the onset of lumen formation, actin was not enriched (green arrows in Fig. 2B). In summary, we conclude that microtubules play an important role in notochord lumen formation.

Actin polymerization is required for lumen formation, maintenance and fusion

Whereas prolonged treatment with latrunculin B blocked not only cell elongation, but also lumen formation (data not shown), the disruption of microtubules produced only a partial block to lumen formation and, concurrently, an ectopic concentration of actin at the presumptive apical domains. These results prompted us to examine in detail the role of actin filaments in lumen formation. We first examined the localization of actin in notochord cells. For this purpose, we developed a fluorescent fusion protein containing the I/LWEQ module of *Ciona* talin A to visualize actin. The talin I/LWEQ module contains an actin-binding domain (Critchley, 2009) that is conserved in *Ciona* talin A and B (which are generated by alternative splicing) (Senetar and McCann, 2005). I/LWEQ modules of both isoforms bind actin in vitro (Singiser and McCann, 2006). *Ciona* talin A I/LWEQ localizes at the cell membrane and is concentrated at focal adhesions when expressed in HeLa cells, whereas talin B I/LWEQ localizes predominantly along stress fibers (Singiser and McCann, 2006). Therefore, talin A I/LWEQ is a potential marker for cortical actin. Immediately before the onset of lumen formation (17.5 hpf), mCherry-talin A I/LWEQ (mCherry-talin A) localized at the basal equatorial domain of the notochord cells and at the lateral junctions, except at the center where the apical domain would emerge (Fig. 6A,A′). These localization signals potentially represent the talin that interacts with integrins at cell-basement membrane and cell-cell junctions. When lumens began to form, a small but significant mCherry-talin A signal was observed in the apical cortical region (white arrows in Fig. 6B,B′), where membrane contacted the emerging lumen. This cortical mCherry-talin A population was juxtaposed with the polarized apical microtubules (Fig. 6C-D′). By 20 hpf, when significant lumen had accumulated, the mCherry-talin A became highly enriched and spanned the entire apical domain, with the strongest signal at the center (Fig. 6E,E′). The presence of an apical cortical actin population during lumen formation was confirmed with two other markers, Lifeact-mEGFP (Vidali et al., 2009) (Fig. 6F,F′) and mCherry-UtrCH (Burkel et al., 2007) (Fig. 6G,G′), and by staining with phalloidin (Fig. 6H,H′).

We next treated the embryos with latrunculin B and blebbistatin at the onset of lumen formation (18 hpf; Fig. 7A). After 2 hours, whereas control embryos produced large lumens (Fig. 7B), no lumens were visible in latrunculin B-treated embryos (Fig. 7C). By contrast, blebbistatin-treated embryos formed normal size lumens (Fig. 7D). We also treated the embryos at 22 hpf, during the lumen formation (Fig. 7E), for 4 hours. Interestingly, whereas extracellular lumens expanded and fused in control and blebbistatin-treated embryos (Fig. 7F,H), lumens in latrunculin B-treated embryos both failed to expand and were significantly reduced in size (white arrows in Fig. 7G). In addition, we examined the cytoskeleton network after drug treatment. As expected, actin filaments were disassembled following latrunculin B treatment from 18-20 hpf (Fig. 7I). Interestingly, and similar to what we observed at the elongation stage, the microtubule network was also severely disrupted (Fig. 7J, compare with Fig. 4C,C′). No polarized concentration of microtubules was observed in the apical cortex; microtubules instead formed thick and disorganized bundles. The cytoskeleton network in blebbistatin-treated embryos was not significantly affected (Fig. 7L-N); both apical cortical actin and microtubules were present. Together with the microtubule disruption phenotype, we conclude that cortical actin and microtubule networks play a concerted role in lumen formation. In contrast to the earlier role of actin in cell elongation, which is myosin II dependent, the role of actin in lumen formation is myosin II independent.

ERM is required for luminal membrane specification and lumen formation

To explore the regulatory mechanism of the apical cytoskeleton in lumen formation, we examined the molecular interaction between membrane and cytoskeleton. We focused on the ERM proteins because they play a crucial role in the organization of membrane domains and the cortical cytoskeleton through their ability to interact with transmembrane proteins and the cytoskeleton (Fehon et al., 2010). ERM proteins contain a N-terminal membrane-

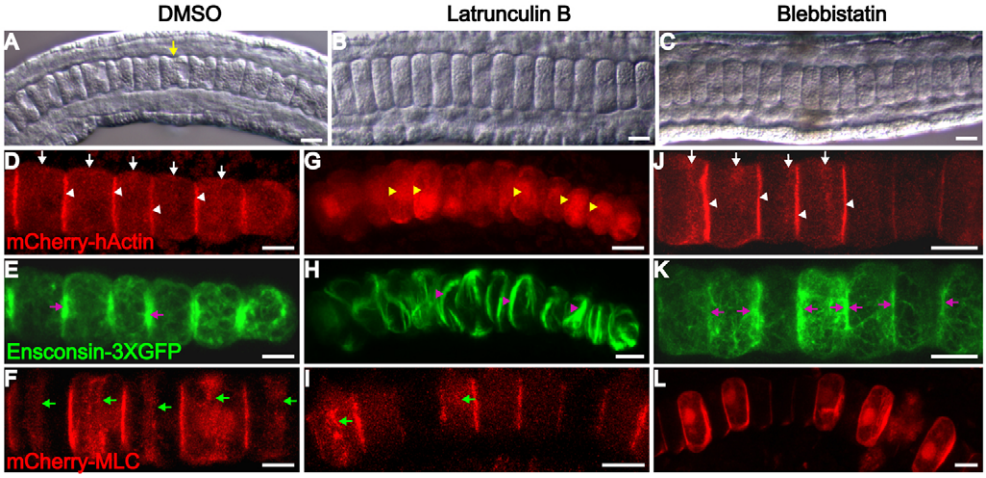

Fig. 3. Actin and non-muscle myosin II are required for basal constriction and cell elongation. (**A-C**) DIC image of notochord in *Ciona* embryos cultured in DMSO (A, control), or treated with 20 μM latrunculin B (B) or 100 μM blebbistatin (C) at 16 hpf for 2 hours. Yellow arrow indicates basal furrow. (**D-L**) Projections of notochord cells labeled with mCherry-hActin (D,G,J), ensconsin-3×GFP for microtubules (E,H,K) or mCherry-MLC (F,I,L), in control (D-F), latrunculin B-treated (G-I) or blebbistatin-treated (J-L) embryos. White arrow indicates circumferential actin ring; white arrowhead indicates actin filaments associated with adherens junctions; yellow arrowhead indicates disorganized actin after latrunculin B treatment; magenta arrow indicates microtubules at prospective apical region; magenta arrowhead indicates abnormal thick microtubule bundles following latrunculin B treatment; and green arrow indicates myosin belt. Scale bars: 10 μm.

associated band 4.1/ezrin/radixin/moesin (FERM) domain, an α-helical region, and a C-terminal ERM-association domain (C-ERMAD) that binds actin (Fehon et al., 2010; Niggli and Rossy, 2008). *Ciona* ERM (Ci-ERM) is specifically expressed in notochord cells at tailbud stages, as shown by in situ hybridization (Hotta et al., 2007) and microarray (data not shown). During lumen formation (21 hpf), we found that Ci-ERM localized at both the lateral domain and apical domain (Fig. 8A, red arrow), in a similar pattern to mCherry-talin A (Fig. 8A′, white arrow), suggesting a role for ERM in lumen formation.

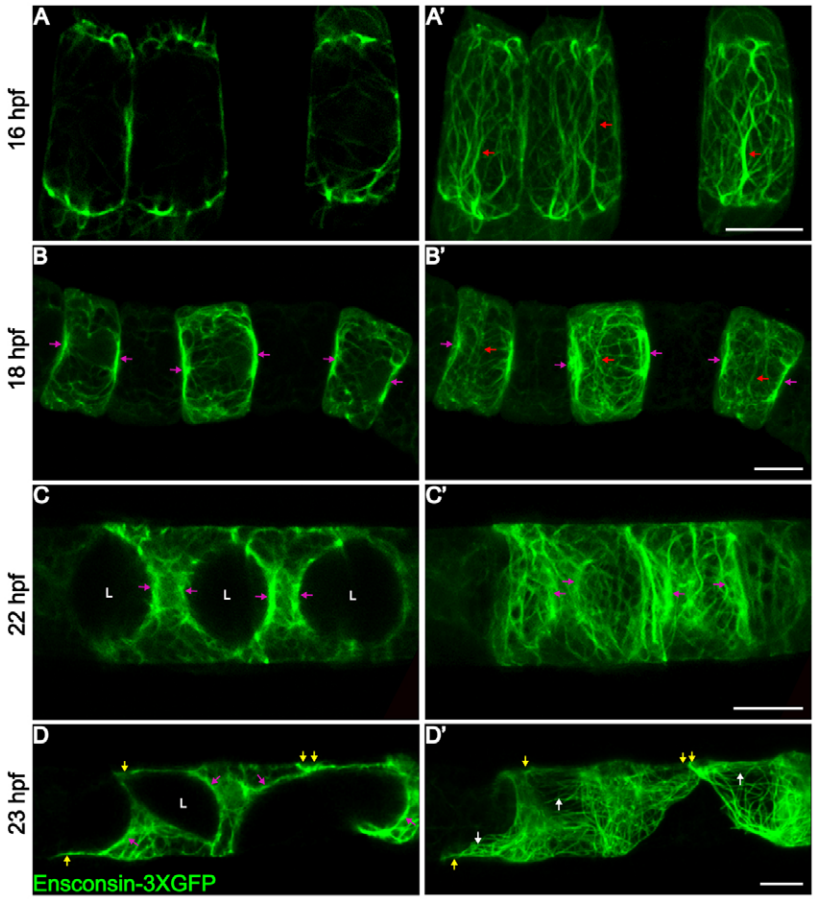

Fig. 4. Localization of microtubule filaments in notochord cells. (**A-D′**) Median confocal sections (A-D) and projections (A′-D′) of *Ciona* notochord cells mosaically labeled with ensconsin-3×GFP at 16 (elongation), 18 (onset of lumen formation), 22 (lumen formation) and 23 (cell movement) hpf. Red arrows indicate microtubules arrayed perpendicularly to the anterior/posterior (A/P) axis; magenta arrow indicates microtubules at prospective (B,B′) or expanding (C-D) apical region; white arrow indicates microtubules parallel to A/P axis; and yellow arrows indicate leading edges of crawling cells. L, lumen. Scale bars: 10 μm.

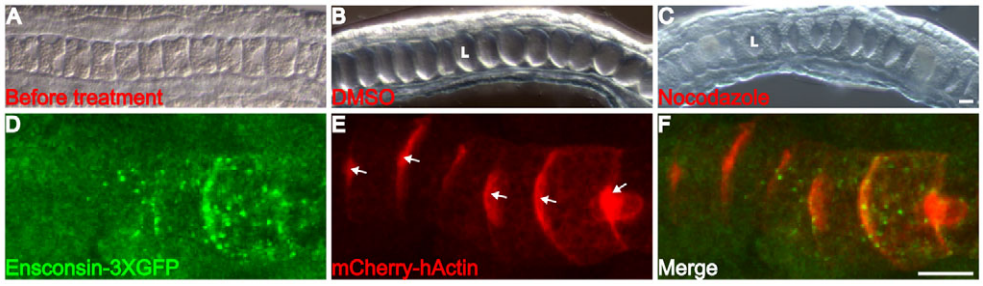

Fig. 5. Depolymerization of microtubule filaments delays notochord lumen secretion and expansion. (**A-C**) DIC images of *Ciona* embryos before (A) and after treatment with DMSO (B) or 40 μM nocodazole (C) from 17.5 to 21.5 hpf. (**D-F**) Projections of notochord cells labeled with ensconsin-3×GFP (D) or mCherry-hActin (E), and merge (F), after 1-hour treatment from 17.5 hpf. White arrow indicates ectopic localization of actin at presumptive apical domain. L, lumen. Scale bars: 10 μm.

To ascertain the function of ERM, we generated a dominant-negative form of Ci-ERM (ERM-DN-tGFP), which contained only the N-terminal 344 amino acids (including the FERM domain), following a previously published example (Allenspach et al., 2001; Amieva et al., 1999) (see Fig. S2 in the supplementary material). Expression of ERM-DN-tGFP had no effect on notochord cell intercalation (Fig. 8B). At 21 hpf, 3 hours after the onset of lumen formation, little or no lumen was visible in notochord cells expressing ERM-DN-tGFP (87%, *n*=64). ERM-DN-tGFP accumulated at the presumptive apical/luminal domain (red arrows in Fig. 8B) and, in cells with small lumens both ERM-DN-tGFP and mCherry-talin A were found at the apical/luminal domain.

We next performed knockdown of ERM using a translation-blocking morpholino (MO) that has been reported to cause a shortened tail phenotype (Hotta et al., 2007). At 22 hpf, notochord in control MO-injected embryos formed large lumens (Fig. 8C; *n*=10), whereas notochord in ERM MO-injected embryos did not form any lumens (Fig. 8D; *n*=19). In addition, we used the protein kinase C (PKC) inhibitor Ro-31-8220, which has been reported to inhibit the phosphorylation of ERM in mouse aortic endothelial cells and to block vascular development (Strilic et al., 2009). We treated the embryos with 50 μM Ro-31-8220 at the onset of lumen formation (18 hpf) for 4 hours. Whereas the notochord in control (DMSO-treated) embryos formed extracellular lumens at 22 hpf (Fig. 8E; 100%, *n*=23), lumen formation in the notochord of drug-treated embryos was significantly blocked (Fig. 8F); only small lumens were occasionally observed (asterisk in Fig. 8F; 36% of embryos had small lumens, 64% no lumen; *n*=36). We conclude that ERM plays an essential role in lumen formation in the *Ciona* notochord.

A rotation of the microtubule network is essential for the orientation of the leading edge protrusion and for lumen fusion

Approximately 4 hours after lumen formation begins, notochord cells form actin-based lamellipodia at their anterior and posterior edges and crawl on the inner surface of the notochordal sheath (Dong et al., 2009) (Fig. 9A). This movement is highly coordinated: each notochord cell eventually produces one anterior and one posterior actin protrusion (Fig. 9B). The protrusive activity at the opposing poles of each cell is required for the merging of the anterior and posterior apical/luminal domains, the change to an endothelial-like cell shape and the fusion of the lumens (Fig. 9C). We observed that at 23 hpf, when notochord cells formed leading edges (yellow arrows in Fig. 4D,D′) and began to crawl, microtubule filaments formed straight and parallel bundles extending to the leading edges (white arrows in Fig. 4D,D′). The orientation of these microtubules was parallel to the A/P axis of the notochord and the direction of the movement of cell edges. This was in contrast to microtubule distribution at earlier stages (16-22 hpf), when the majority of microtubules were oriented perpendicularly to the A/P axis (red and magenta arrows in Fig. 4A′-C′). This 90° rotation of microtubules before lumen fusion suggested that it was involved in the process of cell edge movement. To test this hypothesis, we disrupted microtubules with 40 μM nocodazole at 22 hpf (Fig. 9D). After 4 hours, the control (DMSO-treated) notochord cells became endothelial-like and separate lumens fused (Fig. 9E). In drug-treated embryos, notochord cells began active movement at approximately the same stage as in controls (23 hpf; data not shown). However, the movement was not productive and lumens failed to connect (Fig. 9F). To investigate the underlying mechanism, we examined the distribution of actin filaments and microtubules in nocodazole-treated embryos. As expected, microtubule filaments were efficiently disassembled (Fig. 9J,L). Surprisingly, whereas control notochord cells consistently formed one protrusion at each end (Fig. 9G; *n*=50), drug-treated notochord cells produced multiple protrusions at each end (2.54±0.60 per cell end, *n*=38; three protrusions are shown in Fig. 9I and two in Fig. 9K).

DISCUSSION

We have identified distinct cytoskeleton structures at different stages of notochord tubulogenesis. At the cell elongation stage, a basal actomyosin ring is present at the equator of notochord cells. Microtubules are arranged parallel to the circumferential axis. During lumen formation, both actin and microtubule filaments are assembled at the apical/luminal cortex. When notochord cells begin to crawl bi-directionally along the notochordal sheath in preparation for lumen fusion, actin filaments are enriched in the lamellipodia at the leading edges, and a subset of microtubules extends into the leading edge protrusions. Throughout tubulogenesis, a fraction of actin is associated with adherens junctions at the notochord cell interfaces. We examined the functional significance of some of these cytoskeleton elements in the context of tubulogenesis. Together, our results reveal a temporal and spatial complexity in the cytoskeleton network of the *Ciona* notochord and an extensive crosstalk between different components of the cytoskeleton during tube formation.

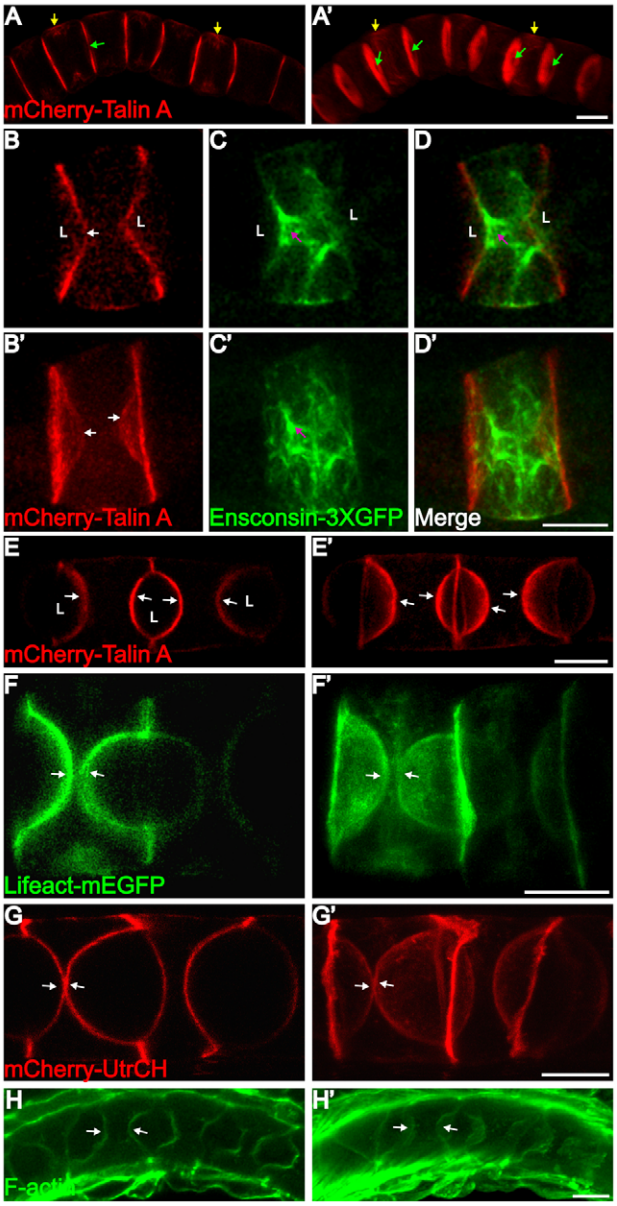

Fig. 6. Actin organization at the apical cortex. (**A**,**A′**) Median confocal section and projection of *Ciona* notochord cells labeled with mCherry-talin A for actin before lumen formation (17.5 hpf). Yellow arrow indicates basal equatorial actin; green arrow indicates prospective apical/luminal domain. (**B-D′**) Median confocal sections (B-D) and projections (B′-D′) of apical/luminal region labeled with mCherry-talin A or ensconsin-3×GFP (for microtubules), and merge, at 19 hpf. White arrow indicates apical actin; magenta arrow indicates apical cortical microtubules. (**E-G′**) Median confocal sections (E-G) and projections (E′-G′) of notochord cells labeled with mCherry-talin A (E,E′), Lifeact-mEGFP (F,F′) or mCherry-UtrCH (G,G′) for actin at 20 hpf. (**H**,**H′**) Median confocal section (H) and projection (H′) of notochord cells stained with phalloidin for F-actin at 20 hpf. White arrow indicates apical cortical actin. L, lumen. Scale bars: 10 μm.

Basal constriction by the actomyosin network as a novel mechanism for cell elongation

Contraction by actomyosin networks is a fundamental mechanism for cell shape changes during development. In the context of cytokinesis, the actomyosin network causes the formation of the cleavage furrow, the ingression of which results in cell cleavage (Rappaport, 1996). The basal equatorial actomyosin machinery we report here bears some resemblance to the cytokinetic contractile ring. It is located at the equatorial region of individual notochord cells and consists of both actin filaments and the motor protein myosin. The activity of this ring is required for the formation of a morphological furrow, as inhibition of its activity resulted in the failure of furrow formation. However, the notochord equatorial actomyosin ring also differs fundamentally from the contractile ring of cytokinesis. First, notochord cells are post-mitotic. Second, we could not detect any significant presence of microtubules in the cytoplasm that might resemble the central spindle or the asters that guide the positioning of equatorial ring (von Dassow, 2009). Importantly, the activity of the actomyosin ring in the notochord cells does not result in complete furrow ingression and cell cleavage. We note that the basal furrow in notochord cells more closely resembles the pseudo-cleavage furrow observed during polarization of the *C. elegans* zygote (Munro et al., 2004). Following the second meiotic division, a dynamic and contractile actomyosin network is preferentially stabilized at the anterior half of the zygote. This asymmetry initiates a flow of myosin and actin filaments towards the anterior pole, while the contraction of the actomyosin network results in a deep invagination resembling a cleavage furrow. This furrow eventually recedes, before the first mitotic spindle forms and mitosis ensues. The asymmetrical stabilization of the actomyosin network and its directional flow are initiated by the polarization activity of PAR proteins. In *Ciona*, several epithelial polarity proteins, including those of the PAR complex, are expressed in notochord cells and are localized in a bipolar fashion (E. Denker and D.J., unpublished). Further experiments are required to examine the role of these proteins in the establishment of the basal equatorial actomyosin ring.

Our study suggests a novel mechanism for cell elongation by the equatorial circumferential contraction of an actomyosin network. We hypothesize, based on the discontinuous localization of non-myosin II, that the actomyosin filaments produce local compressions along the circumference in the cell cortex. The collective outcome of these compressions over a long time scale is to cover the entire circumference and produce constrictive forces at the equator. We suggest that this equatorial constriction is translated by the viscoelastic cytoplasm into a longitudinal force that is exerted on the anterior and posterior edges of the cell to cause elongation (Fig. 10A). Future experiments, including the local disruption of actomyosin contractile elements and the rheological measurement of cytoplasm, will test whether these compressive activities are necessary and sufficient for force generation, furrow formation and cell elongation.

The role of actin and microtubules in notochord extracellular lumen formation

Our study has identified an actin population at the apical cortex of *Ciona* notochord cells during lumen formation. Significantly, this actin population is spatially associated with the cortical microtubules and, together, they form a cytoskeleton network (Fig. 10B). We have shown that both components play a role in lumen formation. Generally, microtubules are responsible for long-distance transport, whereas actin filaments are involved in short-range transport (Goode et al., 2000; Wang and Hsu, 2006). We suggest that in *Ciona* notochord, the luminal vesicles are carried towards the apical membrane along microtubules and that, at the cortex, vesicles switch tracks to actin filaments before arriving at

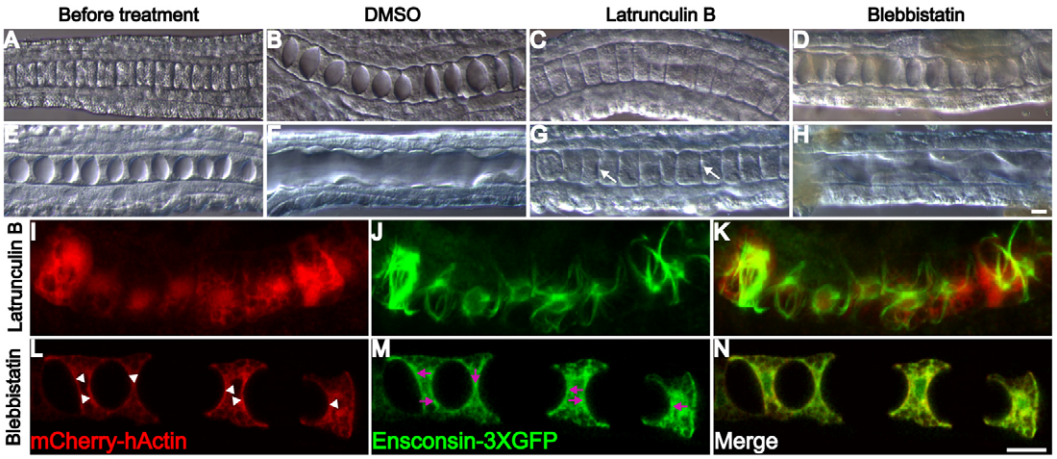

Fig. 7. Actin, but not myosin II, is required for lumen formation, maintenance and fusion. (**A-H**) DIC images of *Ciona* embryos before (A,E) and after treatment with DMSO (B,F), 20 μM latrunculin B (C,G) or 100 μM blebbistatin (D,H) from 18 hpf (onset of lumen formation) for 2 hours (B-D), or from 22 hpf (before cell movement) for 4 hours (F-H). White arrow indicates reduced lumen after latrunculin B treatment. (**I-K**) Projections of notochord cells labeled with mCherry-hActin or ensconsin-3×GFP, and merge, after latrunculin B treatment from 18-20 hpf. (**L-N**) Median confocal section of notochord cells labeled with mCherry-hActin or ensconsin-3×GFP, and merge, after blebbistatin treatment from 18-20 hpf. White arrow indicates apical cortical actin; magenta arrow indicates microtubules at the apical region. Scale bars: 10 μm.

the apical membrane for fusion. Interestingly, inhibition of actin resulted in a much more pronounced effect than the inhibition of microtubules. This could be due to an incomplete disassembly of microtubules, although we think that this is unlikely because at 40 μM, nocodazole efficiently disrupted microtubules at the lumen formation stage (Fig. 5D) and completely blocked lumen fusion (Fig. 9F). Actin filament disassembly by latrunculin B also severely disrupted the microtubules (Fig. 7J), and this might have had an additive disruptive effect on lumen formation. By contrast, the nocodazole treatment resulted in an increase, instead of a loss, of apical actin, which might have compensated for the microtubule defect. In addition, the special morphology of notochord cells during lumen formation might render lumen secretion more dependent on a short-range actin-based transport mechanism. The cytoplasm of each notochord cell between the two apical domains becomes significantly compressed as the neighboring lumens enlarge (Fig. 7E). Ultrastructural analysis of notochord cells at this stage in the ascidian *Ascidia callosa* (Cloney, 1964) and in *Ciona* (our unpublished results) shows that both the Golgi apparatus and rough endoplasmic reticulum are positioned next to the apical domains. Hence, the dependence on microtubules for long-range transport might not be as great as in other luminal epithelial cell types. Our finding is also consistent with an alternative hypothesis that proposes that actin and microtubule filaments form coherent tracks that transport nascent membrane and lumen matrix towards the apical domain. This scenario has been described in the anastomosis of tracheal cells in the *Drosophila* embryo, during which fusion cells form tracks containing F-actin, microtubules and Shot, a plakin that crosslinks F-actin and microtubules, and use these tracks to target intracellular vesicles towards the existing apical surface (Lee and Kolodziej, 2002). Further experiments should reveal whether actin and microtubules work sequentially or more coherently in lumen matrix trafficking in *Ciona* notochord cells.

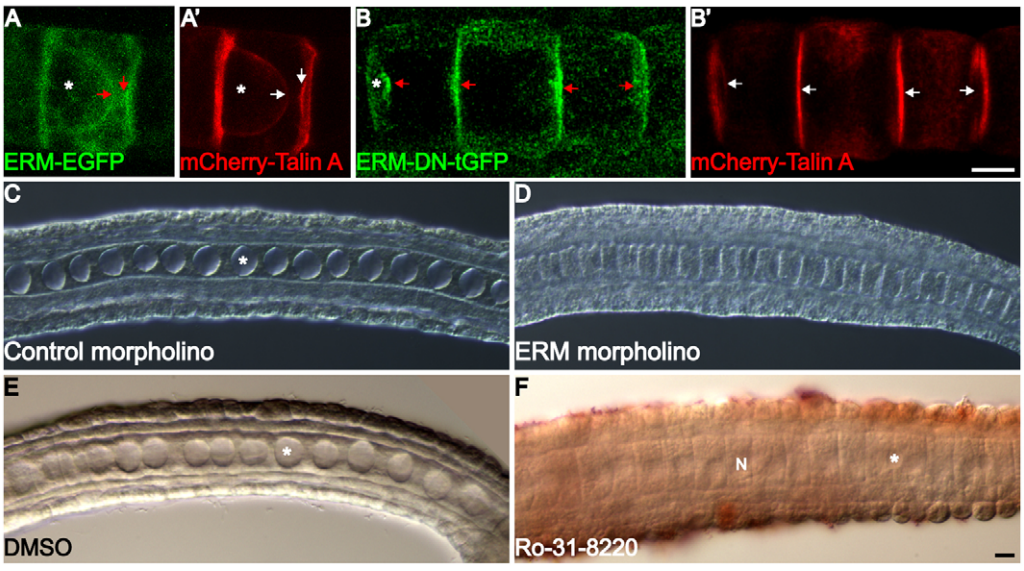

Fig. 8. Ci-ERM is required for luminal membrane specification and lumen formation. (**A**,**A′**) Projection of a representative notochord cell co-expressing ERM-EGFP and mCherry-talin A at 21 hpf. (**B**,**B′**) Projection of notochord cells co-expressing ERM-DN-tGFP and mCherry-talin A at 21 hpf. Red arrow indicates apical ERM; white arrow indicates apical actin. (**C**,**D**) DIC image of *Ciona* embryo injected with control or ERM MO at 22 hpf. (**E**,**F**) DIC image of embryos treated with DMSO or 50 μM Ro-31-8220 at 18 hpf for 4 hours. Asterisk indicates lumen. N, nucleus. Scale bars: 10 μm.

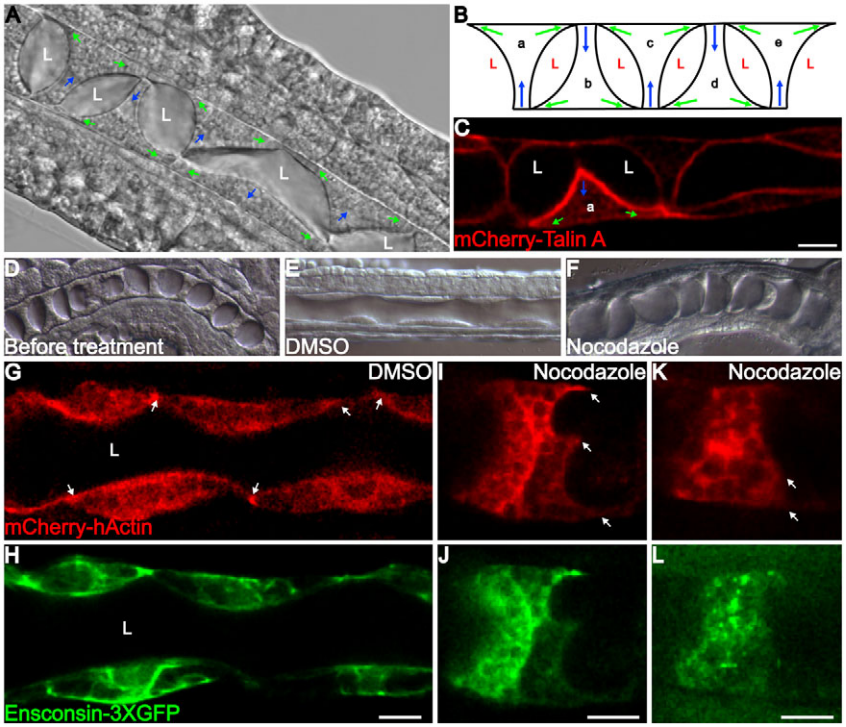

Fig. 9. Microtubule filaments are required for the orientation of leading edge protrusions and for lumen fusion. (**A**) Lumens connecting as a result of notochord cell movement at 24 hpf. (**B**) Model describing the collective movement of five notochord cells (a-e) that results in lumen joining. (**C**) Confocal section of a notochord cell (a) labeled with mCherry-talin A for apical cortical actin at 25 hpf, after merging of anterior and posterior apical domains and fusion of anterior and posterior lumens. Green and blue arrows indicate the direction of leading and trailing edge movement, respectively (see B). (**D-F**) DIC images of *Ciona* embryos before and after treatment with DMSO or 40 μM nocodazole at 22 hpf for 4 hours. (**G-L**) Confocal sections showing the distribution of actin and microtubules in control (G,H) and nocodazole-treated (I-L) embryos at 25 hpf. White arrows indicate protrusions in the notochord cell. L, lumen. Scale bars: 10 μm.

Secretory vesicles have not been visualized in *Ciona* notochord cells. A recent study has revealed a molecular network for the generation of apical membrane and lumen in the MDCK (Madin-Darby canine kidney) cell system. This network includes a PAR3-aPKC complex, exocyst complex, Rab family small GTPases and CDC42 (Bryant et al., 2010). Preliminary experiments show that a PAR3-aPKC complex, Rab5, Rab11 and syntaxin 6 are also localized in *Ciona* notochord cells in a polarized fashion during lumen formation (B.D. and D.J., unpublished). These proteins will serve as useful markers to visualize luminal vesicles and to further study the role of the cytoskeleton network in lumen formation.

In *Ciona* notochord cells, both the disruption of actin polymerization and the inhibition of myosin II activity before lumen formation (16 hpf) blocked cell elongation and extracellular lumen formation. By contrast, at the onset of lumen formation (18 hpf), only the disruption of actin polymerization blocked lumen formation. These results have two implications. First, lumen formation in notochord cells is actin filament assembly dependent but myosin II independent. Second, the cell elongation process is a prerequisite for the lumen formation that follows. This scenario differs from the tight coupling between cell elongation and lumen formation observed in the terminal cell of the tracheal system in *Drosophila* (Gervais and Casanova, 2010). It is, however, similar to a recent observation in VEGFA-deficient mice showing that myosin II fails to be recruited to endothelial cell contacts during aorta tubulogenesis, and that endothelial cells cannot undergo the cell shape changes that normally precede lumen formation (Strilic et al., 2009).

The role of ERM in lumen formation

In this study we provide strong evidence for a requirement of ERM in lumen formation. ERM has been demonstrated to be essential for apical membrane specification and secondary lumen expansion during villus morphogenesis in mouse (Saotome et al., 2004) and for apical membrane biogenesis and lumen morphogenesis of multiple tubular organs in *C. elegans* (Gobel et al., 2004). Our results suggest that the role of ERM in lumen formation is evolutionarily conserved.

The dominant-negative ERM that we used retained the FERM domain that binds transmembrane protein, but lacked the ERMAD domain that interacts with actin filaments. It functions as a dominant-negative by competing for transmembrane proteins with endogenous ERM. It is therefore paradoxical that actin filaments were still localized at the presumptive apical domain in ERM-DN-tGFP-expressing cells (Fig. 8B′). A similar observation has been made in *C. elegans* intestine, in which the cortical actin, which is required for lumen formation, is not displaced from the luminal membrane by *erm-1* RNAi treatment (Gobel et al., 2004). These findings suggest that an alternative mechanism, possibly involving the remodeling of adhesion, regulates the apical accumulation of actin filaments.

Microtubules provide guidance for the organization of actin-based protrusions, which are essential for notochord cell crawling and lumen fusion

We observed that during notochord cell movement, microtubules form parallel bundles that extend towards the leading edges of lamellipodia (Fig. 10C). The reorganization of microtubules that we observed might result from a passive bending of pre-existing filaments in response to the cell shape changes caused by actin protrusions. However, our data suggest a more active role for microtubules in regulating lamellipodia formation. Disruption of microtubules caused multiple lamellipodia to form. It has been shown that the formation of new cell protrusions, including lamellipodia, requires new membrane biogenesis and the assembly of new adhesions. The microtubules that extend into newly protruding regions deliver materials for new membrane and adhesion apparatuses (Balasubramanian et al., 2007; Bretscher and Aguado-Velasco, 1998; Gauthier et al., 2009). In this case,

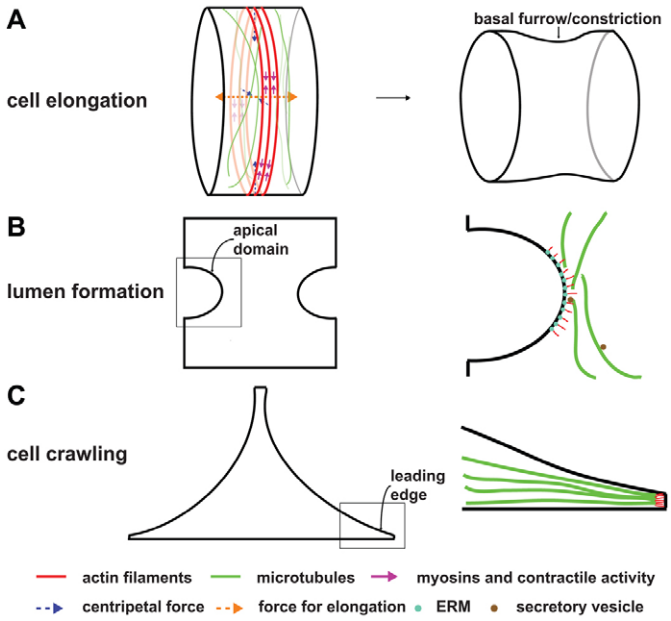

Fig. 10. Models for cytoskeleton organization and contribution at three stages of notochord tubulogenesis in *Ciona*. (**A**) Actin and myosin II form an actomyosin network at the equatorial region of the basal cortex. The contractile activity of this network generates compressions along the cell circumference and causes a furrow to form at the equator. The basal contractions presumably produce centripetal forces, which are converted to pushing forces exerted on both the anterior and the posterior surfaces of a notochord cell, driving the cell to elongate. (**B**) Apical cortical actin, together with juxtaposing microtubules, transport luminal vesicles that contribute to lumen formation. ERM is essential for luminal membrane specification and lumen formation. (**C**) Microtubules form bundles and extend to the leading edges of lamellipodia as notochord cells crawl. Microtubule extension at the cell edge might mechanically provide a positional cue for the orientation of protrusions.

disruption of microtubules might block cell extension instead of causing more protrusions to form. Our finding is also inconsistent with a role for microtubules in the delivery of signaling proteins, including Rac GTPase, which locally activates actin filament growth and membrane protrusion (Waterman-Storer et al., 1999). Alternatively, microtubule polymerization or bundling can directly provide force at the plasma membrane, such as that shown to facilitate neurite initiation (Dehmelt et al., 2006). Microtubule rotation has been implicated in cell elongation and cell shape change in epithelial cells of *Drosophila* (Pope and Harris, 2008). It remains to be addressed whether the pioneering forces generated by microtubule extension mechanically provide positional cues for the orientation of protrusions, thereby guiding cells to crawl directionally on a substrate.

Interaction between actin filaments and microtubules during notochord tubulogenesis

In this study, the roles of actin filaments and microtubules in cell shape change, extracellular lumen formation and cell movement are distinctly defined. However, significant crosstalk exists between these cytoskeleton elements during notochord tubulogenesis. Whenever actin polymerization was inhibited, the organization of microtubules was disrupted. This suggests that actin filaments are essential for the organization of the microtubule network during notochord tube formation. Conversely, disruption of microtubules led to an ectopic accumulation of actin filaments at the apical domains at the onset of lumen formation and to a disorganization of actin-based protrusions at the cell movement stage. Intricate interaction between actin filaments and microtubules occurs in many cellular processes during development. The coordination of actin and microtubule networks can be accomplished directly by common motors or linker proteins (Huang et al., 1999; Lee and Kolodziej, 2002; Wu et al., 2008), or can be mediated indirectly by signaling molecules, such as Rho GTPases (Rodriguez et al., 2003). Future work is needed to identify these structural proteins and regulatory molecules in the context of notochord tubulogenesis.

Acknowledgements

We thank W. C. Smith, E. Denker, A. Roure, P. Lemaitre, R. O. McCann, W. M. Bement, M. Bezanilla and H. Takahashi for providing plasmids, morpholino and other reagents; Mary Laplante for critical reading of the manuscript; and Birthe Mathiesen for animal collection. This work was supported by grants 133335/V40 and 183302/S10 from the Norwegian Research Council to D.J.

Competing interests statement

The authors declare no competing financial interests.

Supplementary material

Supplementary material for this article is available at
http://dev.biologists.org/lookup/suppl/doi:10.1242/dev.057208/-/DC1

References

Allenspach, E. J., Cullinan, P., Tong, J., Tang, Q., Tesciuba, A. G., Cannon, J. L., Takahashi, S. M., Morgan, R., Burkhardt, J. K. and Sperling, A. I. (2001). ERM-dependent movement of CD43 defines a novel protein complex distal to the immunological synapse. *Immunity* **15**, 739-750.

Amieva, M. R., Litman, P., Huang, L., Ichimaru, E. and Furthmayr, H. (1999). Disruption of dynamic cell surface architecture of NIH3T3 fibroblasts by the N-terminal domains of moesin and ezrin: in vivo imaging with GFP fusion proteins. *J. Cell Sci.* **112**, 111-125.

Baer, M. M., Chanut-Delalande, H. and Affolter, M. (2009). Cellular and molecular mechanisms underlying the formation of biological tubes. *Curr. Top. Dev. Biol.* **89**, 137-162.

Balasubramanian, N., Scott, D. W., Castle, J. D., Casanova, J. E. and Schwartz, M. A. (2007). Arf6 and microtubules in adhesion-dependent trafficking of lipid rafts. *Nat. Cell Biol.* **9**, 1381-1391.

Barr, F. A. and Gruneberg, U. (2007). Cytokinesis: placing and making the final cut. *Cell* **131**, 847-860.

Bretscher, M. S. and Aguado-Velasco, C. (1998). Membrane traffic during cell locomotion. *Curr. Opin. Cell Biol.* **10**, 537-541.

Bryant, D. M. and Mostov, K. E. (2008). From cells to organs: building polarized tissue. *Nat. Rev. Mol. Cell Biol.* **9**, 887-901.

Bryant, D. M., Datta, A., Rodriguez-Fraticelli, A. E., Peranen, J., Martin-Belmonte, F. and Mostov, K. E. (2010). A molecular network for de novo generation of the apical surface and lumen. *Nat. Cell Biol.* **12**, 1035-1045.

Burkel, B. M., von Dassow, G. and Bement, W. M. (2007). Versatile fluorescent probes for actin filaments based on the actin-binding domain of utrophin. *Cell Motil. Cytoskeleton* **64**, 822-832.

Chung, S. and Andrew, D. J. (2008). The formation of epithelial tubes. *J. Cell Sci.* **121**, 3501-3504.

Cloney, R. A. (1964). Development of the ascidian notochord. *Acta Embryol. Morphol. Exp.* **7**, 111-130.

Critchley, D. R. (2009). Biochemical and structural properties of the integrin-associated cytoskeletal protein talin. *Annu. Rev. Biophys.* **38**, 235-254.

Dehmelt, L., Nalbant, P., Steffen, W. and Halpain, S. (2006). A microtubule-based, dynein-dependent force induces local cell protrusions: Implications for neurite initiation. *Brain Cell Biol.* **35**, 39-56.

Dong, B., Horie, T., Denker, E., Kusakabe, T., Tsuda, M., Smith, W. C. and Jiang, D. (2009). Tube formation by complex cellular processes in Ciona intestinalis notochord. *Dev. Biol.* **330**, 237-249.

Etienne-Manneville, S. (2004). Actin and microtubules in cell motility: which one is in control? *Traffic* **5**, 470-477.

Fehon, R. G., McClatchey, A. I. and Bretscher, A. (2010). Organizing the cell cortex: the role of ERM proteins. *Nat. Rev. Mol. Cell Biol.* **11**, 276-287.

Foe, V. E. and von Dassow, G. (2008). Stable and dynamic microtubules coordinately shape the myosin activation zone during cytokinetic furrow formation. *J. Cell Biol.* **183**, 457-470.

Gauthier, N. C., Rossier, O. M., Mathur, A., Hone, J. C. and Sheetz, M. P. (2009). Plasma membrane area increases with spread area by exocytosis of a GPI-anchored protein compartment. *Mol. Biol. Cell* **20**, 3261-3272.
Gervais, L. and Casanova, J. (2010). In vivo coupling of cell elongation and lumen formation in a single cell. *Curr. Biol.* **20**, 359-366.
Gobel, V., Barrett, P. L., Hall, D. H. and Fleming, J. T. (2004). Lumen morphogenesis in C. elegans requires the membrane-cytoskeleton linker erm-1. *Dev. Cell* **6**, 865-873.
Goode, B. L., Drubin, D. G. and Barnes, G. (2000). Functional cooperation between the microtubule and actin cytoskeletons. *Curr. Opin. Cell Biol.* **12**, 63-71.
Hirokawa, N., Noda, Y., Tanaka, Y. and Niwa, S. (2009). Kinesin superfamily motor proteins and intracellular transport. *Nat. Rev. Mol. Cell Biol.* **10**, 682-696.
Hogan, B. L. and Kolodziej, P. A. (2002). Organogenesis: molecular mechanisms of tubulogenesis. *Nat. Rev. Genet.* **3**, 513-523.
Hotta, K., Yamada, S., Ueno, N., Satoh, N. and Takahashi, H. (2007). Brachyury-downstream notochord genes and convergent extension in Ciona intestinalis embryos. *Dev. Growth Differ.* **49**, 373-382.
Huang, J. D., Brady, S. T., Richards, B. W., Stenolen, D., Resau, J. H., Copeland, N. G. and Jenkins, N. A. (1999). Direct interaction of microtubule- and actin-based transport motors. *Nature* **397**, 267-270.
Jerdeva, G. V., Wu, K., Yarber, F. A., Rhodes, C. J., Kalman, D., Schechter, J. E. and Hamm-Alvarez, S. F. (2005). Actin and non-muscle myosin II facilitate apical exocytosis of tear proteins in rabbit lacrimal acinar epithelial cells. *J. Cell Sci.* **118**, 4797-4812.
Jiang, D. and Smith, W. C. (2007). Ascidian notochord morphogenesis. *Dev. Dyn.* **236**, 1748-1757.
Lee, S. and Kolodziej, P. A. (2002). The plakin Short Stop and the RhoA GTPase are required for E-cadherin-dependent apical surface remodeling during tracheal tube fusion. *Development* **129**, 1509-1520.
Lu, P. and Werb, Z. (2008). Patterning mechanisms of branched organs. *Science* **322**, 1506-1509.
Lubarsky, B. and Krasnow, M. A. (2003). Tube morphogenesis: making and shaping biological tubes. *Cell* **112**, 19-28.
Massarwa, R., Schejter, E. D. and Shilo, B. Z. (2009). Apical secretion in epithelial tubes of the Drosophila embryo is directed by the Formin-family protein Diaphanous. *Dev. Cell* **16**, 877-888.
Miyamoto, D. M. and Crowther, R. J. (1985). Formation of the notochord in living ascidian embryos. *J. Embryol. Exp. Morphol.* **86**, 1-17.
Munro, E., Nance, J. and Priess, J. R. (2004). Cortical flows powered by asymmetrical contraction transport PAR proteins to establish and maintain anterior-posterior polarity in the early C. elegans embryo. *Dev. Cell* **7**, 413-424.
Niggli, V. and Rossy, J. (2008). Ezrin/radixin/moesin: versatile controllers of signaling molecules and of the cortical cytoskeleton. *Int. J. Biochem. Cell Biol.* **40**, 344-349.
O'Brien, L. E., Zegers, M. M. and Mostov, K. E. (2002). Opinion: building epithelial architecture: insights from three-dimensional culture models. *Nat. Rev. Mol. Cell Biol.* **3**, 531-537.
Pollard, T. D. and Cooper, J. A. (2009). Actin, a central player in cell shape and movement. *Science* **326**, 1208-1212.
Pope, K. L. and Harris, T. J. (2008). Control of cell flattening and junctional remodeling during squamous epithelial morphogenesis in Drosophila. *Development* **135**, 2227-2238.
Rappaport, R. (1996). *Cytokinesis in Animal Cells*. Cambridge: Cambridge University Press.
Rodriguez, O. C., Schaefer, A. W., Mandato, C. A., Forscher, P., Bement, W. M. and Waterman-Storer, C. M. (2003). Conserved microtubule-actin interactions in cell movement and morphogenesis. *Nat. Cell Biol.* **5**, 599-609.
Ross, J. L., Ali, M. Y. and Warshaw, D. M. (2008). Cargo transport: molecular motors navigate a complex cytoskeleton. *Curr. Opin. Cell Biol.* **20**, 41-47.
Roure, A., Rothbacher, U., Robin, F., Kalmar, E., Ferone, G., Lamy, C., Missero, C., Mueller, F. and Lemaire, P. (2007). A multicassette Gateway vector set for high throughput and comparative analyses in ciona and vertebrate embryos. *PLoS One* **2**, e916.
Saotome, I., Curto, M. and McClatchey, A. I. (2004). Ezrin is essential for epithelial organization and villus morphogenesis in the developing intestine. *Dev. Cell* **6**, 855-864.
Satou, Y., Imai, K. S. and Satoh, N. (2001). Action of morpholinos in Ciona embryos. *Genesis* **30**, 103-106.
Senetar, M. A. and McCann, R. O. (2005). Gene duplication and functional divergence during evolution of the cytoskeletal linker protein talin. *Gene* **362**, 141-152.
Singiser, R. H. and McCann, R. O. (2006). Evidence that talin alternative splice variants from Ciona intestinalis have different roles in cell adhesion. *BMC Cell Biol.* **7**, 40.
Strilic, B., Kucera, T., Eglinger, J., Hughes, M. R., McNagny, K. M., Tsukita, S., Dejana, E., Ferrara, N. and Lammert, E. (2009). The molecular basis of vascular lumen formation in the developing mouse aorta. *Dev. Cell* **17**, 505-515.
Tsarouhas, V., Senti, K. A., Jayaram, S. A., Tiklova, K., Hemphala, J., Adler, J. and Samakovlis, C. (2007). Sequential pulses of apical epithelial secretion and endocytosis drive airway maturation in Drosophila. *Dev. Cell* **13**, 214-225.
Vidali, L., Rounds, C. M., Hepler, P. K. and Bezanilla, M. (2009). Lifeact-mEGFP reveals a dynamic apical F-actin network in tip growing plant cells. *PLoS One* **4**, e5744.
von Dassow, G. (2009). Concurrent cues for cytokinetic furrow induction in animal cells. *Trends Cell Biol.* **19**, 165-173.
Wang, S. and Hsu, S. C. (2006). The molecular mechanisms of the mammalian exocyst complex in exocytosis. *Biochem. Soc. Trans.* **34**, 687-690.
Waterman-Storer, C. M., Worthylake, R. A., Liu, B. P., Burridge, K. and Salmon, E. D. (1999). Microtubule growth activates Rac1 to promote lamellipodial protrusion in fibroblasts. *Nat. Cell Biol.* **1**, 45-50.
Wu, X., Kodama, A. and Fuchs, E. (2008). ACF7 regulates cytoskeletal-focal adhesion dynamics and migration and has ATPase activity. *Cell* **135**, 137-148.